Powder properties of hydrogenated ball-milled graphite

Zhang, Y.; Wedderburn, J.; Harris, R.; Book, D.

Link to publication on Research at Birmingham portal

Accepted Manuscript

Title: Powder properties of hydrogenated ball-milled graphite

Author: Y. Zhang J. Wedderburn R. Harris D. Book

Please cite this article as: Y.Zhang, J.Wedderburn, R.Harris, D.Book, Powder properties of hydrogenated ball-milled graphite, Materials Research Bulletin http://dx.doi.org/10.1016/j.materresbull.2014.09.024

Powder properties of hydrogenated ball-milled graphite

Y. Zhang*[a], J. Wedderburn[b], R. Harris[b] and D. Book[b]

[a] Applied Chemistry, Waseda University, Tokyo, 162-0041, Japan

[b]Metallurgy and Materials, University of Birmingham, Birmingham, B15 2TT, UK

---
[*] To whom correspondence should be addressed: Email: yinghe.zhang@googlemail.com

Graphical abstract

Abstract

Ball milling is an effective way of producing defective and nanostructured graphite. In this work, the hydrogen storage properties of graphite, ball-milled in a tungsten carbide milling pot under 3 bar hydrogen for various times (0-40 h), were investigated by TGA-Mass Spectrometry, XRD, SEM and Laser Diffraction Particle Size Analysis. For the conditions used in this study, 10 h is the optimum milling time resulting in desorption of 5.5 wt% hydrogen upon heating under argon to 990 °C. After milling for 40 h, the graphite became significantly more disordered, and the amount of desorbed hydrogen decreased. After milling up to 10 h, the BET surface area increased while particle size decreased: however, there is no apparent correlation between these parameters, and the hydrogen storage properties of the hydrogenated ball-milled graphite.

Keywords

1. Introduction

Hydrogen storage is a key technical challenge that needs to be met to allow the introduction of hydrogen energy economies[1]. High-pressure gas cylinders and cryogenic dewars are currently used to store hydrogen in many prototype mobile applications. However, there is great interest in the development of an alternative approach in which solid-state hydrogen materials are used to store hydrogen, as it is possible to greatly increase the volumetric storage density（90~150 kg H_2 m^{-3}）[2]. The principal remaining challenge is to develop materials which have the necessary gravimetric storage density, i.e. which are able to effectively store 6 kg of hydrogen for the ~500 km range of a typical vehicle [3]. Reversible hydrogen capacity should ideally take place on-board a vehicle at 0-150 °C and 1-30 bar. For fast hydrogen cycling, the chemical (or metallic or ionic) bonds between hydrogen and the atoms / molecules of the storage material should be relatively weak. However, in order to achieve a higher hydrogen storage capacity, these bonds should be relatively strong. In addition, it is necessary to take into account cost and safety issues associated with potential hydrogen storage materials. Conventional metal hydrides have high volumetric storage densities (e.g. 115 kg H_2 m^{-3} for LaNi$_5$), but they are heavy and can be rather expensive [2a]. It has been argued that carbon-based media are promising materials for hydrogen storage [4]. Activated carbon (AC) consists of small graphite crystallites and amorphous carbon, and can have high surface areas of up to 3000 m^2 g^{-1}. Although the gravimetric hydrogen storage density can approach that of liquid hydrogen, low temperatures of around 77 K are required [5]. In the case of graphite, it has been reported that the interlayer distance (0.34 nm) is too short for hydrogen molecules to be absorbed [6]. However there are simulations that suggest that at near-ambient conditions, nanostructured graphite with an optimum structure (0.6-0.75 nm for interlayer spacing) may absorb up to 6 wt% hydrogen (-73 °C, 500 bar) [7].

An effective method of producing nanostructured, defective graphite is by ball milling, as shown by Orimo et al [8], who found that graphite milled under 10 bar hydrogen could absorb 7.4 wt % hydrogen. The milling conditions, such as pressure, gas atmosphere and milling mode, all affect the structure of the resulting milled graphite materials and their hydrogen storage properties. Chen et al [9] found that with increasing hydrogen pressure (3-60 bar) during milling, the total amount of absorbed hydrogen decreases. They postulated that at higher pressures, more hydrogen atoms are trapped both at the edges of the graphene sheets and between the interlayers, which suppresses the formation of further defects. Under the same pressure and atmosphere, the amount of hydrogen stored (measured by heating under argon up to 500 °C) was found to be 0.6 wt% using shearing-mode milling, and 2.7 wt% using impact-mode milling [10]. A significant disadvantage of using

graphite to store hydrogen has been the absence of any reversibility. However, Ichikawa et al [11] demonstrated that an addition of lithium hydride (2:1 molar ratio of graphite and LiH) made it possible to achieve reversibility over a number of cycles. In order to significantly extend the cycling lifetime, there is a need to gain a greater understanding of the hydrogen sorption mechanism(s) involved in the ball-milled graphite system, with and without additions[12]. This includes the relationship between the particle size and specific surface area of the milled graphite powder, and its subsequent hydrogen desorption properties [13].   This work investigates the effect of milling conditions on the microstructure, powder characteristics and hydrogen storage properties of graphite ball-milled in hydrogen.

2. Material and methods

2.1. Sample preparation

High-purity graphite powder (Sigma-Aldrich, -325 mesh, >99.99%) was used as the starting material. Milling was carried out using a tungsten carbide (WC) milling pot and milling balls (250 ml milling pot and 49×7 mm diameter WC balls) on a Retsch PM400 Planetary Ball Mill. WC was selected as it is one of the hardest and densest milling media available. During the milling process it is possible that a small amount of contamination, such as either WC or Co (used as a binder in the construction of the WC milling pot) may be introduced into the carbon. Before milling, the high-purity graphite powder was heated up to 200 °C in a vacuum annealing furnace[14]. The dried graphite was loaded and sealed into the milling pot in an argon glove box to prevent oxidation and water adsorption. The mass ratio of milling balls to the sample is 13. The milling was carried out in 3 bar hydrogen. The rotational velocity was 280 rpm, with a sequence of 15 min grinding and 15 min rest (to prevent temperature build-up in the pot). 1 g samples were taken from the milling pot at different milling times (0-40 h) for analysis.

2.2. Materials characterization

X-ray diffraction (Bruker AXS D8 XRD, Cu Kα = 0.154 nm), Scanning Electron Microscopy (Jeol JSM-6060 LV SEM), Brunauer–Emmett–Teller (BET) adsorption examination (Micromeritics, ASAP 2010) for specific surface area measurement and Laser Diffraction Particle Size Analysis (Coulter, LS230: G/0600/08 Fisons Scientific Equipment) of graphite powder in an aqueous glycerol solution were used to characterise the physical properties of the as-received and milled powders. Thermal Gravimetric Analysis

(TGA) (Netzsch TGA 209, 2 °C min^{-1}) and Mass Spectrometry (MS) (Hiden Hal IV) were used to measure the hydrogen desorption properties.

3. Results and discussion

3.1. Structural characterizations

SEM and laser particle size analyses were carried out on the as-received (Fig. 1a) and milled graphite samples. During ball-milling, the graphite particles were reduced in size and the sharp edges found on some particles disappeared. The graphite sample milled for 10 h appeared to exhibit a wider distribution of particle sizes (Fig. 1b) compared to that at 40 h (Fig. 1c). This is supported by the laser diffraction particle size analysis (Fig. 2 and 3). Laser Diffraction Particle Size Analysis showed that the average particle size significantly decreased with milling up to 1-2 h (Fig. 2 and 3). After which, there were only small further decreases for graphite samples milled for 10 and 40 h (Fig. 3), presumably due to agglomeration during milling. Also, after milling up 10 h, the particle size distribution became narrower (Fig. 2).

The variation of specific microsphere external area (S_{exter}), internal area (S_{inter}) and BET area ($S_{BET}=S_{inter}+S_{exter}$) as a function of milling time, are shown in Fig. 4. After milling up to 10 h, the BET area increased to a value of 550 m^{2}g^{-1}. Meanwhile, S_{inter} increased to 200 m^{2}g^{-1} and S_{exter} increased to 350 m^{2}g^{-1}. After 10 h, such areas increased slightly. This is supported by particle size analysis (Fig. 2 and 3), which shows particle size decreasing as S_{exter} increased. This agrees with the results of Shindo et al [15], in which after milling for 20 h, the surface area did not decrease but reached a plateau. During milling (0-10 h), the increase in S_{inter} suggests that micropores have been produced as part of the increased impacts between the surface of the graphite particles and the milling balls. After 10 h, the external area did not change greatly, suggesting increased particle agglomeration. This is consistent with Francke et al [16] who reported that the agglomeration of the small particles increases after milling up to 6 h,..

The as-received graphite is crystalline and has two main diffraction peaks (002) and (004), as shown in Fig. 5. As milling time increased the intensity of the (002) peak continuously decreased, and almost completely disappeared after 40 h milling. This shows that significant amorphisation of the graphite occurred after milling between 10 and 40 h. Orimo et al [8] reported a similar trend, with the intensity of the (002) peak weakening at 2 h and then disappearing after 5 h milling. However, a shift in the (002) peak from 26.7° to 26.6° 2θ [8], was not observed in this work. Such a shift might be explained by the introduction of Fe impurity from the milling media [17].

When graphite was milled for 40 h, low intensity diffraction peaks associated with tungsten carbide (WC) were observed in the 20 - 50° 2θ region. It is most likely that this is due to contamination from the milling media. In previous work [18], it was shown by vibrating sample magnetometry that the ferromagnetic component of milled graphite increased as a function of milling time. If one assumes that this ferromagnetism was only due to Co (rather than any other Co-based phase(s)), then after 40 h milling this would correspond to 0.04 vol % Co [18].

3.2. Hydrogen desorption properties of the milled graphite

MS was simultaneously carried out during a TGA measurement, allowing the amount of desorbed gases to be estimated. The TGA and MS results (Fig. 6) showed that for a graphite sample milled in hydrogen for 40 h, the amount of hydrogen desorbed was about 5.5 wt%, the ratio of hydrogen to methane was relatively low and the onset desorption temperature was about 400 °C. In order to improve the hydrogen storage capability of nanostructured graphite, there is a need to decrease the temperature of hydrogen desorption, increase the amount of hydrogen desorbed, and also reduce the amount of methane release [14].

The maximum amount of hydrogen desorbed was for the sample milled for 10 h (Fig.7). After 40 h the hydrogen-desorption content decreased, and a significant amount of methane was also desorbed.   The BET area and the particle size changed slightly after 10 h (Fig. 3 and 4). In this work, there is no linear correlation between BET area and the amount of hydrogen desorbed /desorption gases.

The high onset hydrogen desorption temperature of above 400 °C (Fig. 6) suggests a chemisorption process rather than physisorption. Therefore the degree of hydrogen uptake should be related to the number of active carbon atoms that are able to react with hydrogen to form C-H bonds, and not just the measureable BET area.

4. Conclusions

This work shows that ball milling of graphite under a hydrogen atmosphere is an effective method of producing nanostructured graphite which is able to store an appreciable amount of hydrogen. Under the conditions used, it was found that 10 h was the optimum milling time to maximize the amount of hydrogen desorbed and minimise methane release, resulting in desorption of 5.5 wt% hydrogen upon heating under argon to 990 °C. Although BET area and particle size changed with milling, no apparent correlation could be

found with the hydrogen storage properties of the hydrogenated milled graphite powder. It cannot be ruled out that impurities (e.g. W and/or Co) from the milling process may also have a role to play, but it was not possible to detect their presence by any of the techniques employed in this study.

Acknowledgements

References

1. (a) Sevilla, M.; Mokaya, R., Energy storage applications of activated carbons: supercapacitors and hydrogen storage. *Energy & Environmental Science* **2014,** *7* (4), 1250-1280; (b) Dutta, S., A review on production, storage of hydrogen and its utilization as an energy resource. *Journal of Industrial and Engineering Chemistry* **2014,** *20* (4), 1148-1156.
2. (a) Züttel, A., Materials for hydrogen storage. *Mater. Today* **2003,** *6* (9), 24-33; (b) Hamilton, C. W.; Baker, R. T.; Staubitz, A.; Manners, I., B-N compounds for chemical hydrogen storage. *Chem. Soc. Rev.* **2009,** *38* (1), 279-293.
3. von Helmolt, R.; Eberle, U., Fuel cell vehicles: Status 2007. *J. Power Sources* **2007,** *165* (2), 833-843.
4. Züttel, A.; Orimo, S., Hydrogen in nanostructured, carbon-related, and metallic materials. *MRS Bull.* **2002,** *27* (9), 705-711.
5. Zhou, L.; Zhou, Y.; Sun, Y., Studies on the mechanism and capacity of hydrogen uptake by physisorption-based materials. *Int. J. Hydrogen Energy* **2006,** *31* (2), 259-264.
6. Ströbel, R.; Garche, J.; Moseley, P.; Jörissen, L.; Wolf, G., Hydrogen storage by carbon materials. *J. Power Sources* **2006,** *159* (2), 781-801.
7. Patchkovskii, S.; Tse, J. S.; Yurchenko, S. N.; Zhechkov, L.; Heine, T.; Seifert, G., Graphene nanostructures as tunable storage media for molecular hydrogen. *Proc. Natl. Acad. Sci. U. S. A.* **2005,** *102* (30), 10439-10444.
8. Orimo, S.; Majer, G.; Fukunaga, T.; Züttel, A.; Schlapbach, L.; Fujii, H., Hydrogen in the mechanically prepared nanostructured graphite. *Appl. Phys. Lett.* **1999,** *75* (20), 3093-3095.
9. Chen, D. M.; Ichikawa, T.; Fujii, H.; Ogita, N.; Udagawa, M.; Kitano, Y.; Tanabe, E., Unusual hydrogen absorption properties in graphite mechanically milled under various hydrogen pressures up to 6 MPa. *J. Alloys. Compd.* **2003,** *354* (1-2), L5-L9.
10. Huang, Z. G.; Calka, A.; Liu, H. K., Effects of milling conditions on hydrogen storage properties of graphite. *Journal of Materials Science* **2007,** *42* (14), 5437-5441.
11. Ichikawa, T.; Fujii, H.; Isobe, S.; Nabeta, K., Rechargeable hydrogen storage in nanostructured mixtures of hydrogenated carbon and lithium hydride. *Appl. Phys. Lett.* **2005,** *86* (24).
12. (a) Zhang, Y.; Book, D., Effect of milling conditions on the purity of hydrogen desorbed from ball-milled graphite *J. Phys. Chem. C* **2011**; (b) Zhang, Y.; Book, D., Hydrogen storage properties of ball-milled graphite with 0.5 wt% Fe. *International Journal of Energy Research* **2011**; (c) Zhang, Y.; Bevan, A.; Book, D., Hydrogen desorption behaviour of a ball-milled graphite - LiBH4 composite. *the Proceedings of 2011 Materials Research Society (MRS) Fall Meeting & Exhibit* **2012**
13. Touzik, A.; Hentsche, M.; Wenzel, R.; Hermann, H., Effect of mechanical grinding in argon and hydrogen atmosphere on microstructure of graphite. *J. Alloys. Compd.* **2006,** *421* (1-2), 141-145.
14. Orimo, S.; Matsushima, T.; Fujii, H.; Fukunaga, T.; Majer, G., Hydrogen desorption property of mechanically prepared nanostructured graphite. *J. Appl. Phys.* **2001,** *90* (3), 1545-1549.
15. Shindo, K.; Kondo, T.; Sakurai, Y., Dependence of hydrogen storage characteristics of mechanically milled carbon materials on their host structures. *J. Alloys. Compd.* **2004,** *372* (1-2), 201-207.
16. Francke, M.; Hermann, H.; Wenzel, R.; Seifert, G.; Wetzig, K., Modification of carbon nanostructures by high energy ball-milling under argon and hydrogen atmosphere. *Carbon* **2005,** *43* (6), 1204-1212.
17. Chen, Y.; Gerald, J. F.; Chadderton, L. T.; Chaffron, L., Nanoporous carbon produced by ball milling. *Appl. Phys. Lett.* **1999,** *74* (19), 2782-2784.
18. Book, D.; Walton, A.; Mann, V.; Langmi, H.; Harris, R., The Safe, Efficient and Economic Large Scale Storage of Hydrogen, Carbon Trust Research. *Development & Demonstration Projects Progress Report* **2005**.
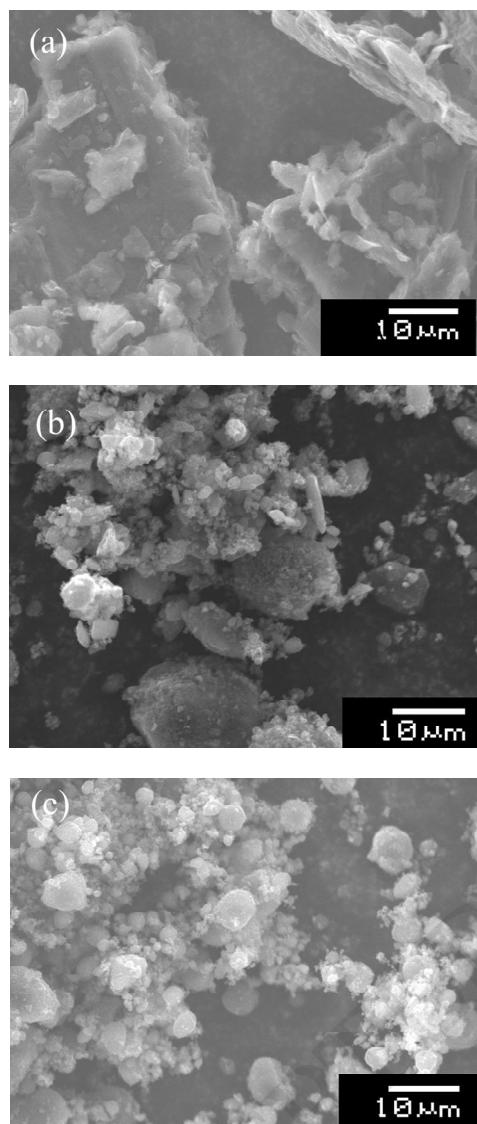
Fig. 1   SEM secondary mode micrographs of: (a) as-received graphite; (b) graphite milled for 10 h; and (c) graphite milled for 40 h (under 3 bar hydrogen).
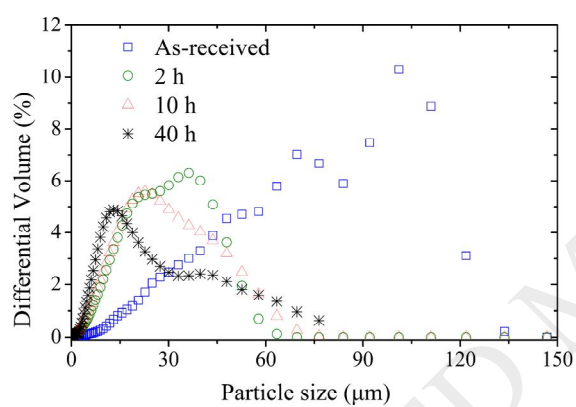
Fig. 2   Distribution of particle size values for as-received graphite (□), and graphite ball-milled in 3 bar hydrogen for 2 h (○), 10 h (Δ) and 40 h (*).
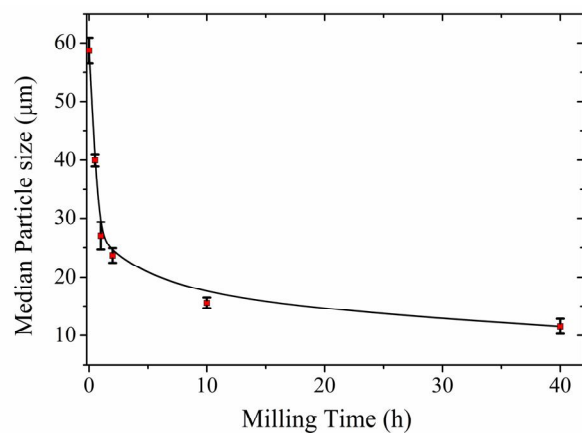
Fig. 3   Laser Diffraction Particle Size Analysis of graphite powder milled for different times (0-40 h) under 3 bar hydrogen
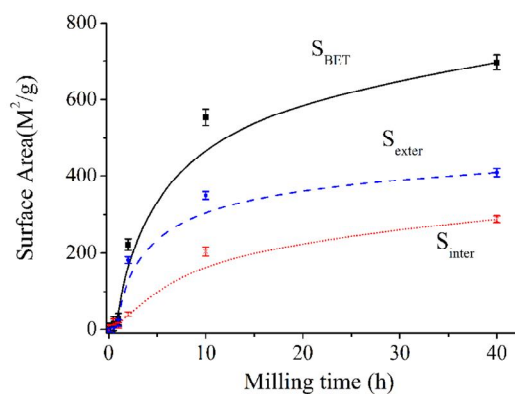
Fig. 4 BET, external, and internal surface areas as a function milling time for graphite powders milled in WC milling media, under 3 bar hydrogen.
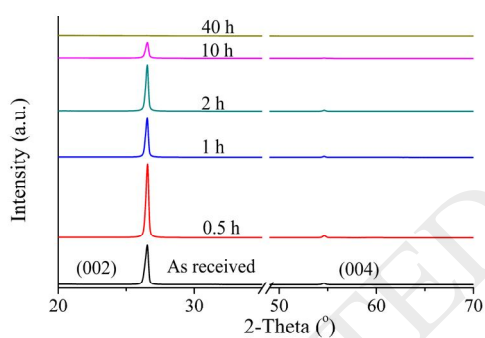

Fig. 5   XRD patterns of graphite milled for various times (0-40 h) under 3 bar hydrogen
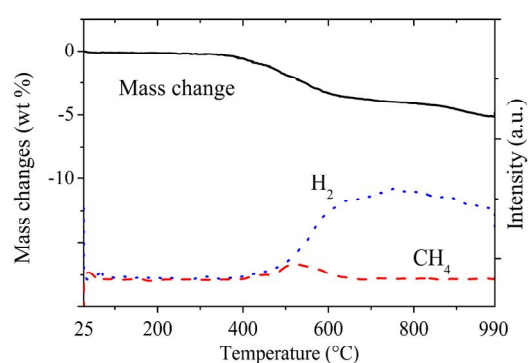
Fig. 6   TGA and mass spectrometry of graphite that had been milled for 40 h in 3 bar hydrogen. Heated at 2 °C/min under 0.5 bar flowing argon.
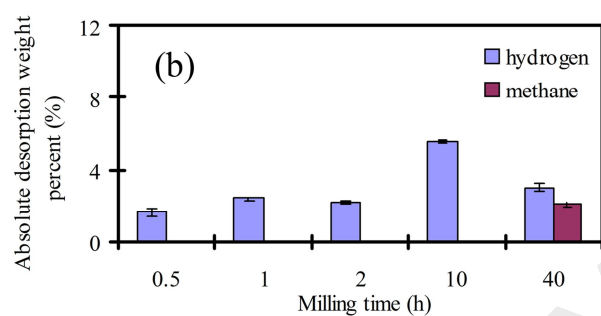

Fig. 7 Amount of hydrogen and methane desorbed from graphite milled under 3 bar hydrogen for various times (0-40 h). Calculated from TGA-MS measurement, e.g. the absolute desorption weight percent for 40 h was estimated from the data in Fig. 6